NASA Technical Memorandum 89060

PREDICTION OF WING AEROELASTIC EFFECTS ON AIRCRAFT LIFT AND PITCHING MOMENT CHARACTERISTICS

CLINTON V. ECKSTROM

OCTOBER 1986

NASA
National Aeronautics and Space Administration

Langley Research Center
Hampton, Virginia 23665

PREDICTION OF WING AEROELASTIC EFFECTS ON AIRCRAFT LIFT AND PITCHING MOMENT CHARACTERISTICS

By Clinton V. Eckstrom
Aerospace Engineer
NASA Langley Research Center
Hampton, Virginia 23665-5225

SUMMARY

The distribution of flight loads on an aircraft structure determines the lift and pitching moment characteristics of the aircraft. When the load distribution changes due to the aeroelastic response of the structure, the lift and pitching moment characteristics also change. An estimate of the effect of aeroelasticity on stability and control characteristics is often required for the development of aircraft simulation models for evaluation of flight characteristics. This presentation outlines a procedure for incorporating calculated linear aeroelastic effects into measured nonlinear lift and pitching moment data from wind tunnel tests. Results are presented which were obtained from applying this procedure to data for an aircraft with a very flexible transport type research wing. The procedure described is generally applicable to all types of aircraft.

LIST OF SYMBOLS

Symbol:	Definition:
C_L	lift coefficient
C_{L_α}	lift coefficient curve slope, per degree
C_{L_H}	horizontal tail lift coefficient
$C_{L_{\delta_H}}$	horizontal tail lift coefficient curve slope, per degree
C_m	pitching-moment coefficient
C_{m_O}	pitching-moment coefficient at zero angle of attack
C_{m_α}	pitching-moment coefficient curve slope, per degree
$C_{m_{\delta_H}}$	horizontal tail pitching-moment coefficient curve slope, per degree
i_H	horizontal tail incidence angle, degrees
m.a.c.	mean aerodynamic chord length, m (in)
q	free stream dynamic pressure, N/m^2 (psf)
S	wing reference area, m^2 (ft^2)
X_A	distance from center of gravity to wing/fuselage aerodynamic center, units of m.a.c., positive forward
$X_H - X_{c.g.}$	distance from center of gravity to horizontal tail aerodynamic center, units of m.a.c., positive aft
α	angle of attack, degrees
α_H	angle of attack at horizontal tail, degrees
$\alpha_{L=O}$	angle of attack at zero lift, degrees
$\alpha_{\epsilon=O}$	angle of attack for zero downwash at tail, degrees
$\Delta\alpha_{L=O}$	incremental change in angle of attack at zero lift, degrees
$\Delta\alpha_{\epsilon=O}$	incremental change in angle of attack for zero downwash at tall, degrees
$\Delta C_{m_{L=O}}$	incremental change in pitching-moment at zero lift, rigid airplane
ΔX_A	incremental change in wing/fuselage aerodynamic center location, units of m.a.c., positive forward
ϵ	downwash angle at horizontal tail, degrees

Symbol:	Definition:
$\epsilon_{\alpha=0}$	downwash angle at zero angle of attack, degrees
δ_H	deflection angle of horizontal tail (elevon), degrees
θ_H	deflection angle of flexible fuselage at horizontal tail station, degress
θ_{HH}	deflection angle of flexible fuselage at horizontal tail station per unit horizontal tail load, radians/lb
$\frac{\partial \epsilon}{\partial \alpha}$	partial of downwash angle with angle of attack, deg/deg

Abbreviations/Superscripts/Subscripts:

CS	cruise shape (wing)
FS	fabrication shape (wing)
TO	tail off

INTRODUCTION

It is well known that aircraft static aeroelastic characteristics can have a significant effect on structural loadings, stability and control characterstics, control surface effectiveness and flight performance characteristics and therefore should be considered during all phases of the vehicle design process. One of the areas where static aeroelastic effects must be considered is in the development of a stability and control data base for use in aircraft simulation models. Such simulation models may be used early in the design process for structural loading evaluations, control law development and evaluation of control capability. The simulation models may also be used for hardware verification, flight plan preparation, and pilot training. Usually the wind tunnel test data on stability and control as well as performance characteristics are obtained from rigid models built to a specific design shape. For a transport type wing the design shape (planform, airfoil shapes, twist distribution, etc.) is usually selected to maximize efficiency at cruise flight conditions whereas for a fighter type aircraft the wing design may be selected for a specific maneuver condition or capability. In either case a structural deflection calculation must be made to define a fabrication shape such that the full scale wing will deform to the desired shape when subjected to the loading expected at the design condition.

For the example described herein the aircraft had a transport type wing for which the given information included (1) the wind tunnel measurements of stability and control characteristics for a rigid model with a cruise shape wing (ref. 1) and (2) the fabrication shape for the full scale wing (ref. 2). What was needed was a prediction of the performance and stability and control characteristics of the full scale aircraft with a flexible wing. The approach was to use a static aeroelastic analysis procedure (ref. 3), which has linear aerodynamic and structural equations, to calculate the aerodynamic characteristics of the aircraft with both a rigid cruise shape wing and a rigid fabrication shape wing and also to do the same calculations for the aircraft with a flexible wing starting in the fabrication shape. The next step was to determine (1) the differences in stability and control characteristics between the rigid cruise shape and the rigid fabrication shape and (2) the changes due to flexibility (aeroelastic effects, defined as a function of flight dynamic pressure). These differences were then applied to the wind tunnel measured data as increments or as ratios to give a nonlinear prediction of the stability and control characteristics for the flexible flight vehicle. The procedure for doing this was developed from and is similar to that of reference 4. The information for the example case presented herein includes the lift and pitching moment characteristics at a Mach number of 0.80, although the calculations were performed for a range of Mach numbers.

AIRCRAFT CHARACTERISTICS

The procedure described was applied to a research wing mounted on a drone vehicle (ref. 5). The size and general arrangement of the research wing and drone vehicle are shown in figure 1. The fuselage is a modified Firebee II target drone vehicle. The research wing was designed for a 2.5-g maneuver load at a gross vehicle weight of 1134 kg (2500-pounds). The wing structural strength and stiffness were determined using an integrated design procedure which included the use of active controls. Wing loading was reduced using maneuver and gust load alleviation. Wing stiffness was reduced using active flutter suppression (ref. 2). Therefore the wing is quite flexible in comparison to most transport type wings in use today. Also inertial effects are small because the wing has no engines, internal fuel, stores, or other large added masses.

A comparison of wing leading edge elevation (droop) and spanwise twist distributions for the wing in both the cruise and fabrication shape is presented in figure 2. The leading edge of the cruise shape wing is a straight line with a very slight downward slope toward the wing tip. The leading edge of the fabrication shape wing droops downward considerably from the cruise shape wing to compensate for the

upward bending that will occur due to the lifting aerodynamic loads experienced at the cruise flight conditions (M = 0.80, C_L = .53, q = 6080 Newtons per square meter (127 psf)). The wing twist distribution for the cruise shape wing (fig. 2) was selected for aerodynamic efficiency reasons relative to spanwise lift distribution and wing tip stall. The fabrication shape wing has a reduced negative twist distribution to compensate for the negative twisting which will occur as a result of bending when the wing is subjected to the aerodynamic loads associated with the cruise flight conditions.

WIND TUNNEL TEST DATA

The wind tunnel tests (ref. 1) were performed on a rigid 0.237-scale model with a cruise shape wing. Data are presented for tests performed at a Mach number of 0.80 with the model in both the tail-on and tail-off configurations. Lift and pitching moment coefficient data are shown in figure 3. The slight difference between the two sets of lift coefficient data results from the lift on the tail. Note that the lift on the tail is downward until an angle of attack of about 6-degrees has been reached. The circles and squares represent actual test data points whereas the solid and dashed lines represent equations which were fit to the test data points. The equations were used to define a set of pseudo "wind tunnel" results such that data at smaller angle of attack increments could be used in subsequent analyses.

For the pitching moment coefficient data (fig. 3) the difference between data for the tail-on and tail-off configurations is considerably greater. The difference is the lift on the tail multiplied by the moment arm length between the tail center of pressure and the vehicle center of gravity (the c.g. is defined as being at 0.25 m.a.c.). Note that the two curves cross at about 6-degrees angle of attack indicating that the lift on the tail changes from negative to positive which is in agreement with the lift coefficient data.

Two additional scale model wind tunnel test measurements are needed to determine downwash at the tail location. They are the horizontal tail lift and pitching moment coefficient curve slopes, per degree deflection. For the example case given these parameters had values of 0.0124 per degree and -0.048 per degree respectively and were assumed to be linear over the angle of attack or horizontal tail deflection angles of interest.

ANALYSIS METHOD

The tasks and procedures for obtaining the predicted lift and pitching moment characteristics for a flexible aircraft are outlined in the flow chart presented in figure 4. The wind tunnel test data for the tail-on and tail-off aircraft configurations referred to on the left side of the chart (fig. 4) have already been presented. The static aeroelastic analyses referred to on the right side of the chart were performed using the Flexible Airplane Analysis Computer Program called FLEXSTAB (ref. 3). As noted on the chart, static aeroelastic analyses are required for: (1) rigid analytical models at both the design cruise shape and the fabrication shape, and (2) a flexible analytical model (initially at the fabrication shape) subjected to various levels of flight dynamic pressure. In each case analysis results are needed for both horizontal-tail-on and horizontal-tail-off aircraft configurations. These linear analysis results are then used to define incremental changes in lift and pitching moment between the two rigid shapes and for the variations of flight dynamic pressure for the flexible model. The incremental changes defined by the linear analysis method are then used either directly, or as ratios, to modify the measured non-linear wind tunnel data using a procedure developed from and similar to that of reference 4.

A basic assumption associated with the prediction procedure is that lift curve intercept changes determined by FLEXSTAB analysis should be applied to the measured wind tunnel data as a shift in angle of attack for zero lift rather than as a change in lift at zero angle of attack. As a result the modified wind tunnel curves are translated along the angle of attack axis with no change in the prediction of maximum lift capability. A second assumption is that the change in lift curve slope for the flexible wing should be proportional to the incremental change in lift. Therefore the correction to be applied to lift curve slope is a function of both dynamic pressure and lift curve slope from the original non-linear lift curve rather than just as a function of dynamic pressure. These assumptions basically define how the prediction procedure is applied as explained in the following sections.

Analysis Results for Lift Coefficient

A comparison of the lift coefficients calculated using the FLEXSTAB analysis procedure is presented in figure 5(a) for the rigid cruise shape wing and the rigid fabrication-shape wing (tail-off aircraft configuration). FLEXSTAB results for lift are in the form of a lift coefficient for zero angle of attack and a lift curve slope from which the angle of attack for lift coefficient equals zero is determined. It is the difference in angle of attack at zero lift (C_L = 0) between calculated results for the cruise shape wing and the fabrication shape wing that is the incremental value to be used in modifying the measured wind tunnel lift coefficients to those expected for the rigid fabrication shape wing. Note that for those two rigid wing shapes there is a shift in angle of attack for zero lift but no change in lift curve slope.

The next step is to calculate the lift coefficient slope and intercept values for the flexible wing (tail-off configuration) using the FLEXSTAB analysis procedure. Lift coefficient slope and intercept values for the flexible wing are shown in figure 5(b).

The effects of flexibility were determined at the various non-zero dynamic pressure values shown. Results for the rigid fabrication shape (fig 5(a)) are presented at zero dynamic pressure for reference purposes as this is the basline condition from which flexibility effects are evaluated. The results for the flexible wing are different from those for the rigid wing shapes in that there is a change in both the slope and intercept values as flight dynamic pressure is changed. The changes in lift curve slope occur because the wing twist distribution for the flexible wing is a function of wing loading which in turn is a function of aircraft angle of attack for any given flight dynamic pressure.

A summary of the calculated incremental changes in angle of attack at zero lift is shown in figure 6. These values are needed as one set of inputs for modifying the measured wind tunnel data to account for the wing rigid shape change, cruise shape to fabrication shape, (shown in figure 6 at zero flight dynamic pressure) and for the aeroelastic effects which are a function of flight dynamic pressure. (These data were obtained from figure 5 at $C_L = 0$). Note that the incremental angle of attack changes for the wing rigid shape change and for the wing flexibility effects are opposite in sign. The fabrication shape wing has zero lift at a larger negative angle of attack than the cruise shape wing because, as shown earlier, the fabrication shape wing has less negative twist along the span than does the cruise shape wing. However as the flight dynamic pressure is increased, the aft swept flexible wing will bend upwards at the tip resulting in an effectively decreasing local angle of attack along the span.

The values of lift curve slopes from figure 5 (b) ratioed to the value of lift curve slope for the rigid case (q = o) are presented in figure 7 as a function of dynamic pressure multiplied by the lift curve slope for the analysis rigid case. The curve defined in figure 7 will be used to determine the ratio by which wind tunnel measured lift curve slopes should be modified or corrected. The abscissa for the data in figure 7 was chosen so that during the modification process, when either the flight dynamic pressure of interest is small, or the slope of the wind tunnel lift curve is small the correction factor, or flexible to rigid ratio, determined from the curve (fig. 7) will be nearer to 1.0 and the modification to the wind tunnel measured lift curve slope will be smaller. In this way the shallow slope of the lift curve (fig. 3) near maximum lift will receive only a very small correction whereas those portions of the lift curve with highest slopes will get the largest corrections.

Analysis Results for Pitching Moment Coefficient

Changing the wind tunnel measured pitching moment coefficient curve to account for wing shape changes is a two step process. The first step is to establish the incremental changes in pitching moment at zero lift as shown in figure 8 for the tail-off aircraft configuration. Pitching moment coefficients as a function of angle of attack calculated for the rigid cruise shape and rigid fabrication shape wings are shown in figure 8(a). Similar results for the flexible wing starting in the fabrication shape are shown in figure 8(b) for several values of flight dynamic pressure. Note that the value of pitching moment for zero lift determined at q = 0 (fig. 8(b)) is the same as for the rigid fabrication shape wing (fig. 8(a)).

A summary of the incremental changes in pitching moment at zero lift are presented in figure 9 as a function of flight dynamic pressure to show the relationship between the increment for changing from the rigid cruise shape wing to the rigid fabrication shape wing (at zero dynamic pressure) and the increments for the flexible wing. Note that the increment between rigid shapes is opposite in sign to the increments due to flexibility.

As previously mentioned, changing the wind tunnel measured pitching moment coefficient curve to account for wing shape changes is a two step process. The first step is to establish the incremental changes in pitching moment at zero lift as shown on figures 8 and 9. The second step is to change the slopes of the pitching moment coefficient curves because of changes in aerodynamic center positions resulting from different wing shapes. Figure 10 presents the incremental changes in aerodynamic center location as a function of flight dynamic pressure resulting from going first from the rigid cruise shape to the fabrication shape, shown at a dynamic pressure of zero, and then for increasing dynamic pressure for the flexible wing. These data were obtained directly from the static aeroelastic analysis results without additional computations. As can be seen the incremental change in aerodynamic center location, due to the wing changing from the rigid cruise shape to the rigid fabrication shape, is negligible in comparison to the changes due to flexibility as dynamic pressure is increased.

Procedure for Modifying Wing Tunnel Data

Lift coefficient is shown plotted in figure 11 versus both angle of attack and pitching moment coefficient to illustrate the first few of several steps in obtaining modified non-linear wind tunnel data. The illustration shown is for changing data from a rigid cruise shape wing to data for a rigid fabrication shape wing. The dashed lines represent wind tunnel measured data for the tail off model configuration. Data points have been selected along the dashed line in increments of 1.0 degree in angle of attack with the exception that the data point at $C_L = 0$ is an interpolated value. Each of these data points also represents a step in the modification process as defined by the i = 0 to i = 8 notation in the center of the figure. The solid lines are the resulting non-linear estimated data for the rigid fabrication shape wing. For lift coefficient versus angle of attack the new data for the rigid fabrication shape wing is simply the measured wind tunnel data (cruise shape wing) shifted over on the angle of attack axis at each data point by the incremental change of angle of attack at zero lift determined

by analysis. This means that each segment between data points on the new curve has exactly the same slope as the original wind tunnel data.

Determining the pitching moment coefficient for the rigid fabrication shape wing is a two step process. The first step is to shift the initial value for pitching moment at zero lift (at i = 0) by the incremental change in pitching moment at zero lift as determined by analysis (fig. 9). The second step is to determine the new incremental values of pitching moment as shown by the equation at the top of figure 11. The new increment in pitching moment for each step, i, along the curve is equal to the increment of the original wind tunnel data plus the product of the incremental change in aerodynamic center, ΔX_A, times the incremental change in lift coefficient for each step. As presented earlier, (fig. 10), there was only a very small change in aerodynamic center in going from the rigid cruise shape wing to the rigid fabrication shape wing, therefore each of the steps along the two pitching moment curves are nearly parallel. The data shown are for values of lift starting at zero and going positive. The same procedure, starting at zero lift and going negative, is used to determine data for the fabrication shape for negative values of lift coefficient.

Introducing flexibility affects (as a function of flight dynamic pressure) into the modification procedure makes changing the lift coefficient curve into a two step process. The first step is to introduce the appropriate incremental change in angle of attack for lift equals zero (fig. 6) similar to what was done for the illustration in figure 11. The second step is to work up the incremental steps (starting from i = 0) in figure 11 by multiplying the wind tunnel measured lift curve slope by the appropriate flexible to rigid ratio for lift curve slope (fig. 7) for each increment and building a new lift coefficient curve in this manner. The procedure for the pitching moment curve remains the same as previously described with the appropriate incremental changes in pitching moment at zero lift and aerodynamic center location coming from figures 9 and 10 respectively.

Lift and pitching moment coefficient results for the flexible airplane in the tail-off configuration are presented in figure 12. Pitching moment is again presented as a function of lift coefficient to show, for the flexible airplane, how the large changes in aerodynamic center affect the slopes of the pitching moment curves. Data for both lift coefficients and pitching moment coefficients are presented for lift coefficient values both greater and less than zero. The plots also show the wind tunnel data for reference purposes. The left side of figure 12 shows how the incremental changes in angle of attack at zero lift coefficient and the changes in lift curve slope with dynamic pressure affect lift coefficient data. The right side of the figure shows how the pitching moment coefficient changes with the rigid shape change and with increasing dynamic pressure for the flexible wing.

Tail Effects

Predictions of wing aeroelastic effects on lift and pitching moment characteristics were also made for the tail-on aircraft configuration. A description of the procedure (ref. 4) used to determine these effects is presented in the Appendix. Figure 13 presents the flow downwash angle at the horizontal tail as derived from measured wind tunnel data by a procedure also described in the Appendix. The flow downwash angle at the horizontal tail is also effected by the rigid and flexible wing shape changes. These effects, which are estimated using the linear static aeroelastic analysis, primarily result in shifting the curve of figure 13 along the horizontal axis but there are also some moderate slope changes that result from wing flexibility. The changes which occur to both the angle of attack at which the downwash angle is zero (intercept) and the rate of change of downwash angle with change in angle of attack (slope) are presented in figure 14. As can be seen from the curve for the intercept, the incremental change resulting from going from the rigid cruise shape wing to the rigid fabrication shape wing (shown at dynamic pressure of zero) is larger in the positive direction than the negative increments for the range of dynamic pressure shown. The changes in slope as a function of flight dynamic pressure are very small. Note that the symbols used on the right half of figure 14 correspond to the dynamic pressure values used on the left half of the figure.

Analysis results are presented in figure 15 for the airplane with a flexible wing but a rigid fuselage in the tail-on configuration, i.e., where the tail effects have been added as a part of the computation process. Note also that the pitching moment coefficient data are now presented as a function of angle of attack. The wind tunnel measured data for the rigid cruise shape wing are again included for reference purposes. The data for lift coefficient looks very similar to that for the tail-off configuration as the lift on the tail does not significantly change the total lift. However, the effect of the tail loading on pitching moment is very significant as was shown earlier in figure 3. Note that the reversal in the pitching moment curve between two and six degrees angle of attack smoothes out considerably at the higher dynamic pressure flight conditions.

Fuselage Flexibility Effects

Comparisons of pitching moment coefficients predicted for the airplane with a flexible wing in the tail-on configuration are presented in figure 16 for calculations which both neglected and included fuselage flexibility. Fuselage flexibility effects the angle of attack at the tail and therefore effects the contribution of the tail to the pitching moment coefficient. Although the fuselage flexibility effect is small in this case, it is still noticeable particularly for the higher angles of attack and dynamic pressures.

Inertia Effects

Because the example wing has no engines, internal fuel, stores or other large added masses the inertial relief effects were found to be negligible. Therefore the analysis for the flexible analytical model were performed at zero angle of attack for all dynamic pressures. If wing masses are large and inertial effects significant it may be necessary to perform the analysis in a piece-wise linear fashion to account for variations in g-loadings with angle of attack and dynamic pressure conditions.

CONCLUDING REMARKS

- Wind tunnel measurements of aircraft stability and control characteristics are usually made on a rigid model with the wing shaped for the design condition.
- If flexibility is significant the wing for a full scale aircraft will be built to a fabrication shape which accounts for the deformation expected at design flight conditions.
- Stability and control characteristics for the full scale aircraft should match wind tunnel measured data at the design flight condition but may be significantly different at off-design flight conditions.
- A procedure has been presented for using static aeroelastic analysis results to modify measured wind tunnel data to account for aeroelastic effects at different flight conditions.
- Example results for lift and pitching moment characteristics for a highly flexible transport type wing were presented which show significant changes with dynamic pressure because of flexibility effects.

APPENDIX - ANALYSIS OF TAIL EFFECTS

Analysis of wing shape change and wing flexibility effects for the tail-off aircraft configuration was rather straightforward. Unfortunately, the tail-on aircraft configuration complicates matters considerably, particularly when fuselage flexibility effects on horizontal tail angle are included. The analysis of tail effects is presented in two parts. The first part is an analysis of tail effects for a rigid wing shape change, i.e., in going from the rigid cruise shape wing to the rigid fabrication shape wing (the fuselage is also considered to be rigid). The second part is an analysis of tail effects for the addition of both wing and fuselage flexibility although, as was done in the text, the flexibility effects can be treated separately.

Tail Effects for a Rigid Wing Shape Change

Downwash at Tail: In order to determine the contribution of the horizontal tail to lift and pitching moment characteristics it is necessary to calculate the flow downwash angle at the horizontal tail location. This can be done by comparing moment equations for tail-off and tail-on configurations.

$$C_{m_{TO}} = C_{m_{O_{TO}}} + C_{m_{\alpha_{TO}}} \cdot \alpha \qquad \text{TAIL-OFF} \qquad (1)$$

$$C_m = C_{m_O} + C_{m_\alpha} + C_{m_{\delta_H}} \cdot \delta_H \qquad \text{TAIL-ON} \qquad (2)$$

When the effective angle of attack at the tail (α_H) is zero then the tail load $C_{m_{\delta_H}} \cdot \delta H$ is zero and $C_{m_{T_O}} = C_m$. Setting equations (1) and (2) equal and solving for α, as a function of δ_H, at which α_H is zero,

$$\alpha = \frac{C_{m_O} - C_{m_{O_{TO}}} + C_{m_{\delta_H}} \cdot \delta_H}{C_{m_{\alpha_{TO}}} - C_{m_\alpha}} \qquad (3)$$

The horizontal tail angle of attack, α_H is

$$\alpha_H = \alpha - \varepsilon + i_H + \theta_H + \delta_H \qquad (4)$$

The tail incidence angle, i_H, for the example aircraft is zero and the body bending term, θ_H, is not applicable for the rigid case (flexibility will be added later). Equation (4) for the rigid vehicle is

$$\alpha_H = \alpha - \varepsilon + \delta_H \qquad (4a)$$

Rearranging for downwash angle, ε, when $\alpha_H = o$,

$$\varepsilon = \alpha + \delta_H \qquad (5)$$

Equation (5) is valid for all α but δ_H must correspond with zero tail load, i.e., $\alpha_H = o$.

$$\frac{\partial \varepsilon}{\partial \alpha} = 1 + \frac{\partial \delta_H}{\partial \alpha} \qquad (6)$$

Going back to equation (3) and differentiating with respect to α and solve for $\frac{\partial \delta_H}{\partial \alpha}$

results in

$$\frac{\partial \delta_H}{\partial \alpha} = \frac{C_{m_{\alpha_{TO}}} - C_{m_\alpha}}{C_{m_{\delta_H}}} \tag{7}$$

Substituting (7) into (6) to get $\frac{\partial \varepsilon}{\partial \alpha}$,

$$\frac{\partial \varepsilon}{\partial \alpha} = 1 + \frac{C_{m_{\alpha_{TO}}} - C_{m_\alpha}}{C_{m_{\delta_H}}} \tag{8}$$

Finding δ_H for $\alpha = o$ and no tail load from equation (3)

$$\delta_{H_{\alpha=o}} = \frac{C_{m_{o_{TO}}} - C_{m_o}}{C_{m_{\delta_H}}} \tag{9}$$

and substituting into (5) to get ε for $\alpha = o$.

$$\varepsilon_{\alpha=o} = \frac{C_{m_{o_{TO}}} - C_{m_o}}{C_{m_{\delta_H}}} \tag{10}$$

$$\varepsilon = \varepsilon_{\alpha=o} + \frac{\partial \varepsilon}{\partial \alpha}\,\alpha \tag{11}$$

This procedure for determining downwash angle, ε, as a function of angle of attack, α, is used for both the wind tunnel data and the FLEXSTAB analysis results. In each case it requires data for both the tail-off and tail-on aircraft configurations. A comparison should be made of the downwash determined using FLEXSTAB data with downwash determined using wind tunnel data to assure that there is a good correlation. For the fabrication shape wing the incremental change in angle of attack for zero downwash is:

$$\alpha_{\varepsilon=o} = -\frac{\varepsilon_{\alpha=o}}{\partial \varepsilon / \partial \alpha} \tag{12}$$

$$\Delta\alpha_{\varepsilon=o} = (\alpha_{\varepsilon=o})_{FS} - (\alpha_{\varepsilon=o})_{CS} \tag{13}$$

The inputs for equations (12) and (13) come from FLEXSTAB runs tail-off and tail-on for both the cruise shape and fabrication shape wings. The curve for ε versus α determined from evaluation of wind tunnel data (figure 13) is now translated along the angle of attack axis by the increment $\Delta\alpha_{\varepsilon=o}$ (figure 14) to obtain a new curve of modified wind tunnel data for the fabrication shape wing.

Horizontal Tail Loads: Wind tunnel data must be evaluated to determine the lift coefficient for the horizontal tail, C_{L_H}, as a function of angle of attack at the tail, α_H. The angle of attack at the tail is determined for the fabrication shape wing using equation (4a) and the new values of ε for the fabrication shape wing.

Lift Coefficient (Tail On): The lift coefficient for the rigid fabrication shape wing is

$$C_L = C_{L_{TO}} + C_{L_H} \tag{14}$$

Pitching Moment Coefficient (Tail On): The pitching moment coefficient for the rigid fabrication shape wing is

$$C_m = C_{m_{TO}} - C_{L_H} \cdot (X_H - X_{CG}) \tag{15}$$

Tail Effects for a Flexible Wing and Fuselage

The fabrication shape flight wing and the flight vehicle fuselage are both flexible structures and therefore subject to deformation from aerodynamic and inertial loading. The analysis procedure presented here accounts for only the deformation due to aerodynamic loading (no inertial loading).

Downwash at the Tail: The procedure for determining the effects of the flexible wing shape changes on downwash at the tail are essentially the same as for the rigid wing shape changes discussed earlier. However when the flexibility of the fuselage is included in the analysis there are additional terms to consider. Start again by comparing moment equations for tail-on and tail-off configurations.

$$C_{m_{TO}} = C_{m_{o_{TO}}} + C_{m_{\alpha_{TO}}} \cdot \alpha \tag{16}$$

$$C_m = C_{m_o} + C_{m_\alpha} \cdot \alpha + C_{m_{\delta_H}} \cdot \delta_H \tag{17}$$

When the effective angle of attack at the tail, α_H, is zero, then the tail load $C_{M_{\delta_H}} \cdot \delta_H$ is zero, $C_{m_{TO}} = C_m$ and we can equate (16) and (17) and solve for α, as a function of δ_H, at which α_H is zero.

$$\alpha = \frac{C_{m_O} - C_{m_{O_{TO}}} + C_{m_{\delta_H}} \cdot \delta_H}{C_{m_{\alpha_{TO}}} - C_{m_\alpha}} \tag{18}$$

The angle of attack at horizontal tail, α_H, is

$$\alpha_H = \alpha - \varepsilon + i_H + \theta_H + \delta_H \tag{19}$$

From equation (18) α_H is zero and for the example aircraft the all moveable horizontal tail has no incidence angle i_H. Solving for downwash angle ε,

$$\varepsilon = \alpha + \delta_H + \theta_H \tag{20}$$

where θ_H is body bending angle at horizontal tail. Body bending θ_H is a function of:

$$\theta_H = \theta_{H_{\alpha=O}} + \frac{\delta\theta_H}{\partial\alpha}\,\alpha + \frac{\partial\theta_H}{\partial\delta_H}\,\delta_H \tag{21}$$

We now need FLEXSTAB runs with the tail on at α=o and α=o to get $\theta_{H_{\alpha=O}}$ and $\frac{\partial\theta_H}{\partial\alpha}$

Body deflection, at the horizontal tail, due to incremental load due to tail deflection, δ_H, is:

$$\Delta\theta_H = C_{L_{\delta_H}} \cdot S \cdot q \cdot (\delta_H + \theta_H)\theta_{HH} \tag{22}$$

where θ_{HH} is the diagonal element of the free-free structural influence coefficient matrix for the fuselage at the horizontal tail attachment point.

Solving equation (22) for θ_H and differentiating with respect to δ_H results in

$$\frac{\partial\theta_H}{\partial\delta_H} = \frac{C_{L_{\delta_H}} \cdot S \cdot q \cdot \theta_{HH}}{1 - C_{L_{\delta_H}} \cdot S \cdot q \cdot \theta_{HH}} \tag{23}$$

Now subsituting equation (23) into equation (21) and equation (21) into equation (20) results in an equation for downwash at the tail, ε, where the values for the parameters are obtained from FLEXSTAB runs.

$$\varepsilon = \theta_{H_{\alpha=O}} + \left(1 + \frac{\partial\theta_H}{\partial\alpha}\right)\alpha + \left[\frac{1}{1 - C_{L_{\delta_H}} \cdot S \cdot q \cdot \theta_{HH}}\right]\delta_H \tag{24}$$

Equation (24) is valid for all α but δ_H must correspond with zero tail load.

$$\frac{\partial\varepsilon}{\partial\alpha} = 1 + \frac{\partial\theta_H}{\partial\alpha} + \left[\frac{1}{1 - C_{L_{\delta_H}} \cdot S \cdot q \cdot \theta_{HH}}\right]\frac{\partial\delta_H}{\partial\alpha} \tag{25}$$

Going back to equation (18) and differentiating with respect to α and solving for $\frac{\partial\delta_H}{\partial\alpha}$ results in

$$\frac{\partial\delta_H}{\partial\alpha} = \frac{C_{m_{\alpha_{TO}}} - C_{m_\alpha}}{C_{m_{\delta_H}}} \tag{26}$$

Substitiuting (26) into (25) results in

$$\frac{\partial\varepsilon}{\partial\alpha} = 1 + \frac{\partial\theta_H}{\partial\alpha} + \frac{C_{m_{\alpha_{TO}}} - C_{m_\alpha}}{C_{m_{\delta_H}}\left(1 - C_{L_{\delta_H}} \cdot S \cdot q \cdot \theta_{HH}\right)} \tag{27}$$

Now finding δ_H for α = o and no tail load from equation (18)

$$\delta_{H_{\alpha=O}} = \frac{C_{m_{O_{TO}}} - C_{m_O}}{C_{m_{\delta_H}}} \tag{28}$$

and substituting into (24) to get ε for α = o

$$\varepsilon_{a=o} = \theta_{H_{\alpha=O}} + \frac{C_{m_{O_{TO}}} - C_{m_O}}{C_{m_{\delta_H}}\left(1 - C_{L_{\delta_H}} \cdot S \cdot q \cdot \theta_{HH}\right)} \tag{29}$$

Equations (27) and (29) describe the downwash ε as a function of α

$$\varepsilon = \varepsilon_{\alpha=O} + \frac{\partial\varepsilon}{\partial\alpha} \cdot \alpha$$

Horizontal Tail Loads: For the flexible vehicle configuration the angle of attack at the horizontal tail includes the effect of fuselage bending.

$$\alpha_H = \alpha - \varepsilon + i_H + \theta_H + \delta_H \tag{30}$$

where $\theta_H = \theta_{H_O} + \frac{\partial \theta_H}{\partial \alpha} \cdot \alpha + \theta_{HH} \cdot C_{L_{\alpha_H}} \cdot \alpha_H \cdot q \cdot S$ (31)

The assumption is made that θ_{H_O} and $\frac{\partial \theta_H}{\partial \alpha}$ are for the tail-off configuration and that all body bending due to tail loads is contained in the last term. Rearranging equations (30) and (31) and solving for α_H yields

$$\alpha_H = \frac{\alpha \left(1 + \frac{\partial \theta_H}{\partial \alpha}\right) - \varepsilon + i_{H_O} + \theta + \delta_H}{\left(1 - \theta_{HH} \cdot C_{L_{\alpha_H}} \cdot q \cdot S\right)} \tag{32}$$

For the example aircraft $i_H = o$ and for these cases the elevon deflection δ_H is also set to zero. Therefore

$$\alpha_H = \frac{\alpha \left(1 + \frac{\partial \theta_H}{\partial \alpha}\right) - \varepsilon + \theta_{H_O}}{\left(1 - \theta_{HH} \cdot C_{L_{\alpha_H}} \cdot q \cdot S\right)} \tag{33}$$

Lift Coefficient (Tail On): The lift coefficient for the flexible wing and vehicle is

$$C_L = C_{L_{TO}} + C_{L_{\alpha_H}} \cdot \alpha_H \tag{34}$$

Pitching Moment Coefficient (Tail On): The pitching moment coefficient for the flexible wing and vehicle is

$$C_m = C_{m_{TO}} - C_{L_{\alpha_H}} \cdot \alpha_H \cdot (X_H - X_{c.g.}) \tag{35}$$

REFERENCES

1. Byrdsong, Thomas A.; and Brooks, Cuyler W., Jr.: Wind-Tunnel Investigation of Longitudinal and Lateral-Directional Stability and Control Characteristics of a 0.237-Scale Model of a Remotely Piloted Research Vehicle With a Thick High-Aspect-Ratio Supercritical Wing, NASA TM-81790, July 1980.

2. Staff of Boeing Wichita Company: Integrated Design of a High Aspect Ratio Research Wing With an Active Control System for Flight Tests on a BQM-34F Drone Vehicle, NASA CR-166108, June 1979.

3. Hink, G. R.; Snow, R. N.; Bhatia, K. G.; Maier, R. E.; Bills, G. R.; Henderson, D. M.; Bailey, D. C.; Dornfield, G. M.; and Dauria, P. V.: A Method For Predicting the Stability and Control Characteristics of an Elastic Airplane. Volume II FLEXSTAB 1.02.00 Users Manual, NASA Contract NAS2-5006, NASA CR-114713, Oct. 1974.

4. Letsinger, G. R.; and Lewis, G. E.: APTI-F-111 Stability and Control Report, Revision D, The Boeing Company, Document No. D365-10041-1, August 1983.

5. Murrow, H. N.; and Eckstrom, C. V.: Drones for Aerodynamic and Structural Testing (DAST) - A Status Report, Journal of Aircraft, Volume 16, Number 8, August 1979.

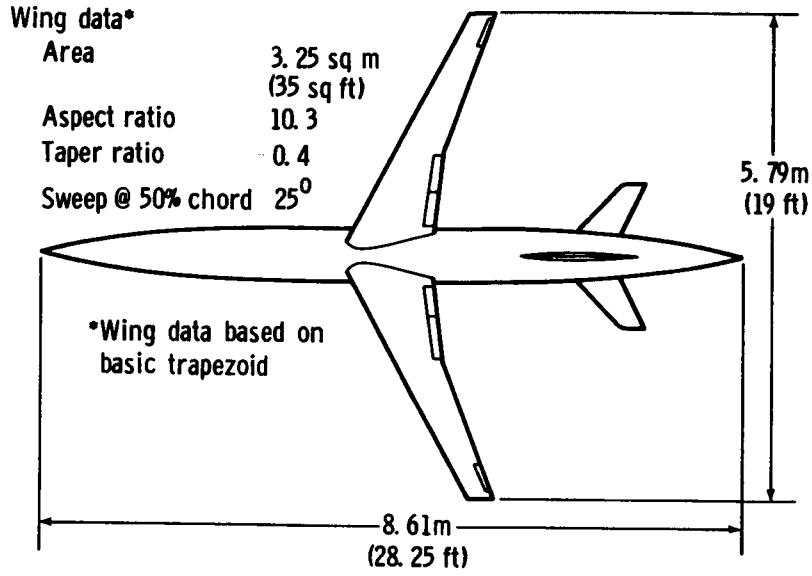

Figure 1.-Aircraft used as example problem.

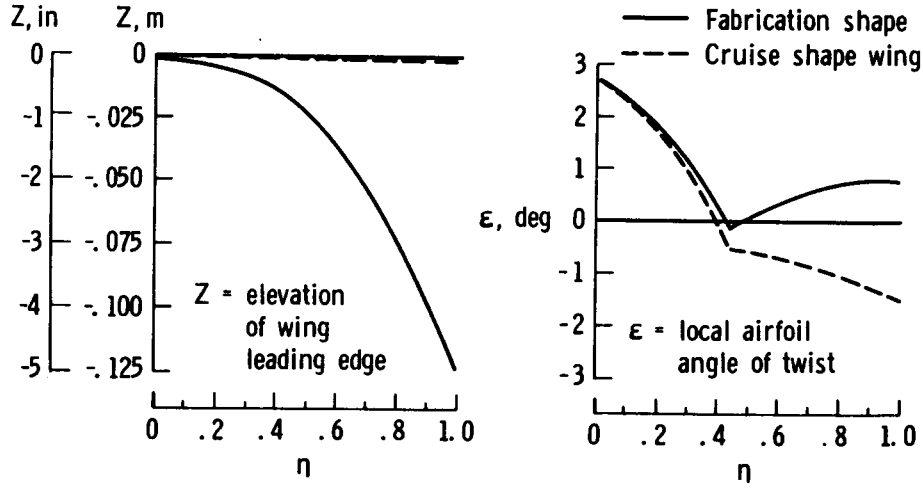

Figure 2.-Comparisons of wing droop and twist distributions for cruise and fabrication shape wings.

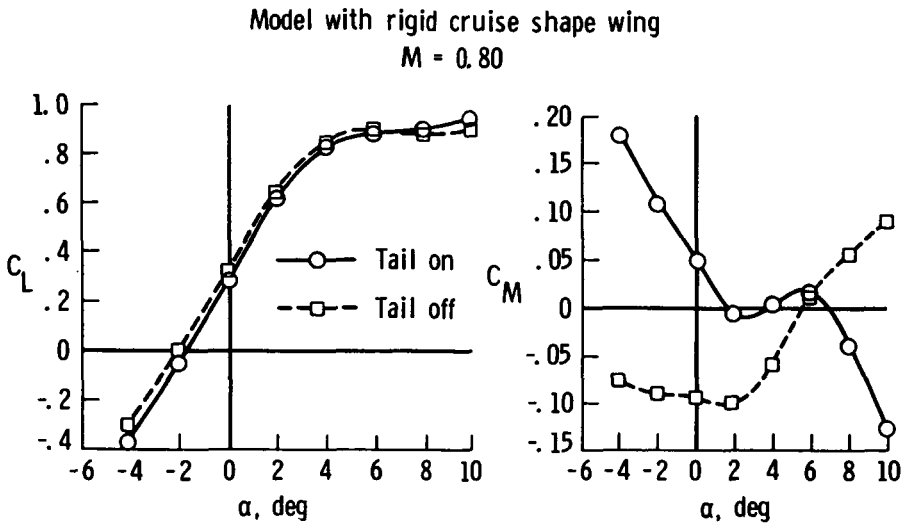

Figure 3.-Lift and pitching moment coefficient data from wind tunnel test.

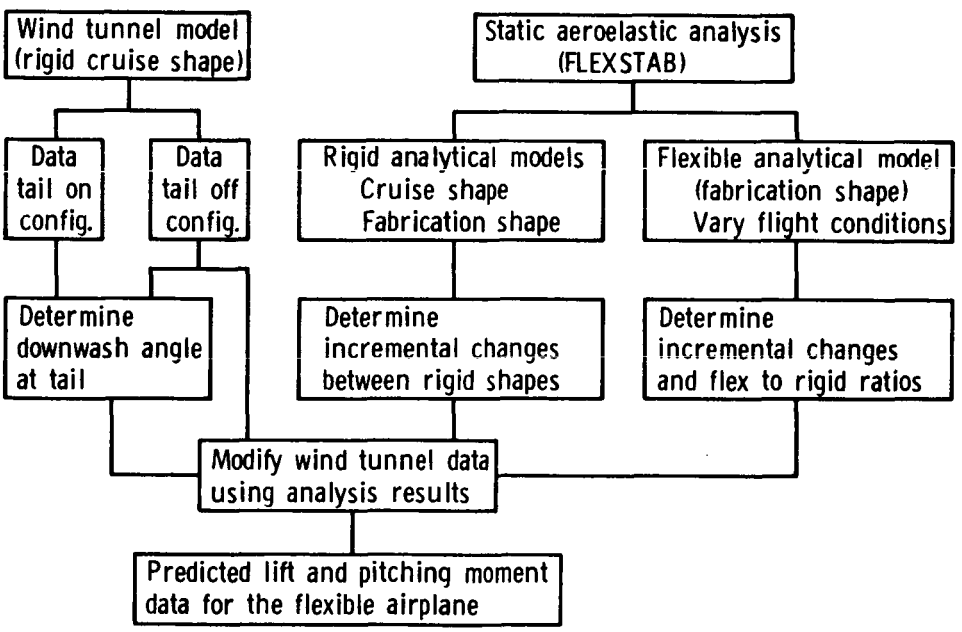

Figure 4.-Flow chart showing analysis procedure.

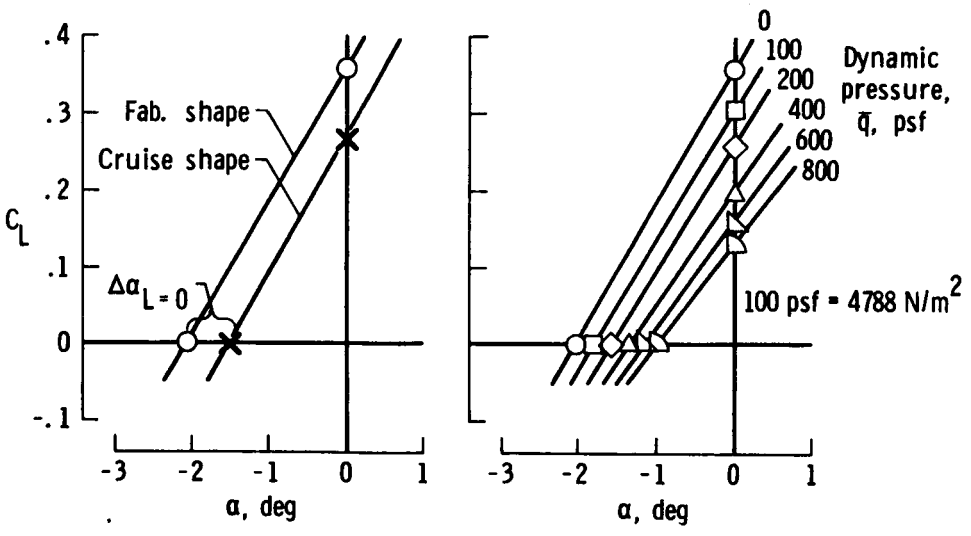

a) Rigid shape change effect. b) Flexibility effects.

Figure 5.-Static aeroelastic analysis of lift characteristics.

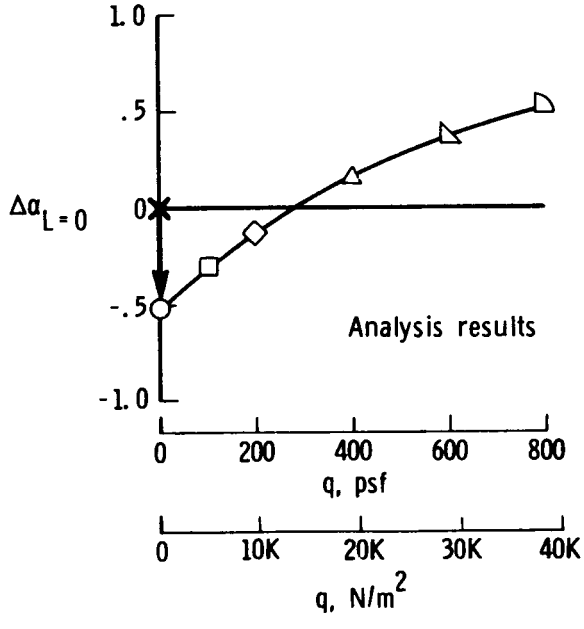

Figure 6.-Incremental changes in angle of attack at zero lift.

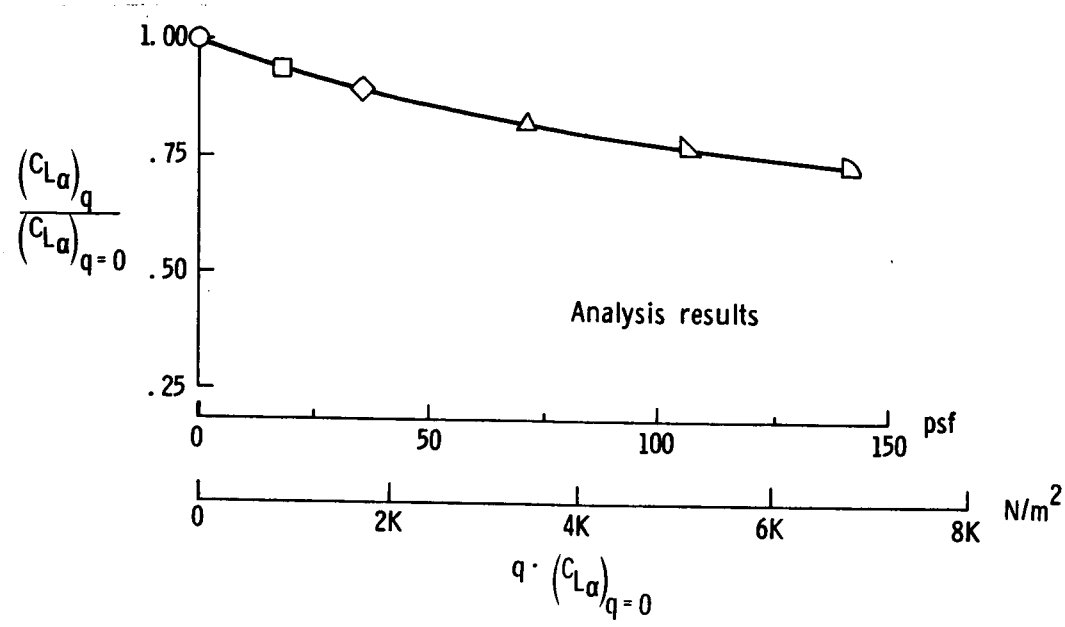

Figure 7.-Ratio of flexible to rigid lift curve slopes.

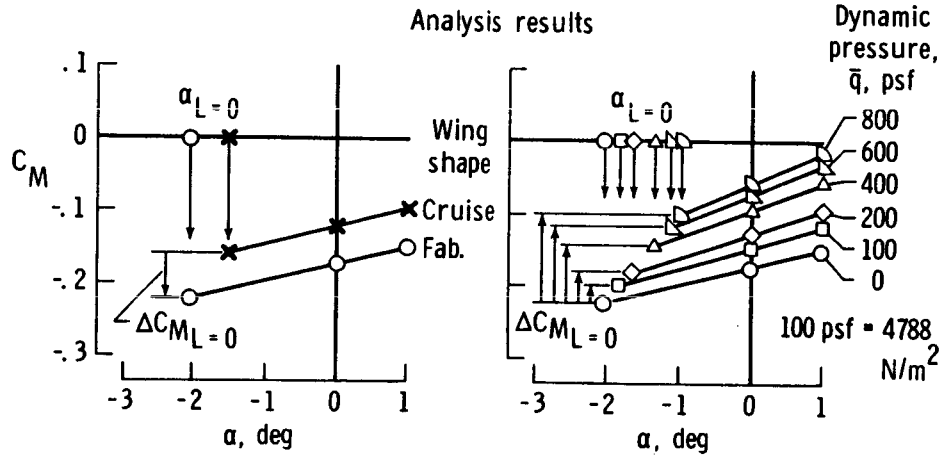

a) Rigid shape change effect. b) Flexibility effects.

Figure 8.-Change in pitching moment cofficient at zero lift.

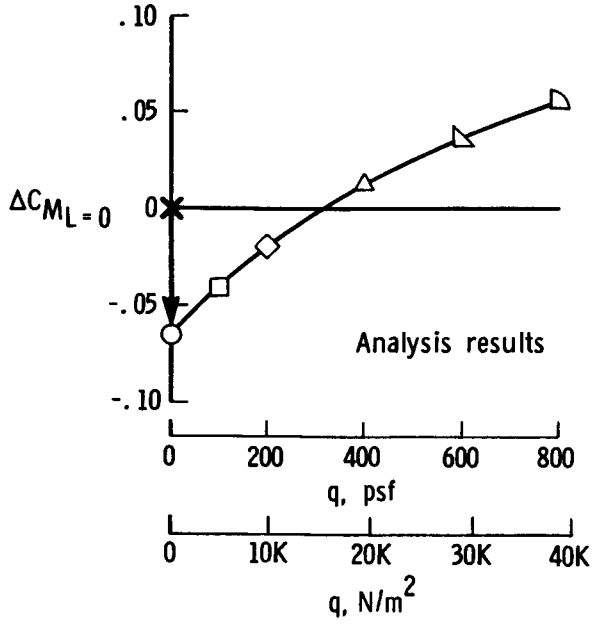

Figure 9.-Incremental changes in pitching moment coefficient at zero lift.

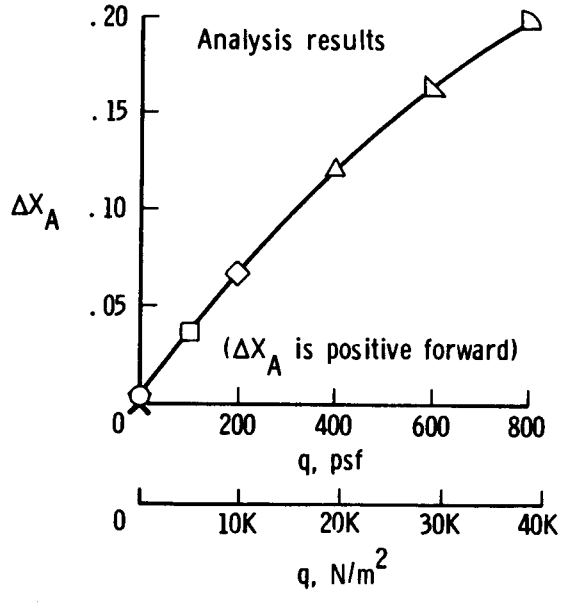

Figure 10.-Incremental changes in aerodynamic center location.

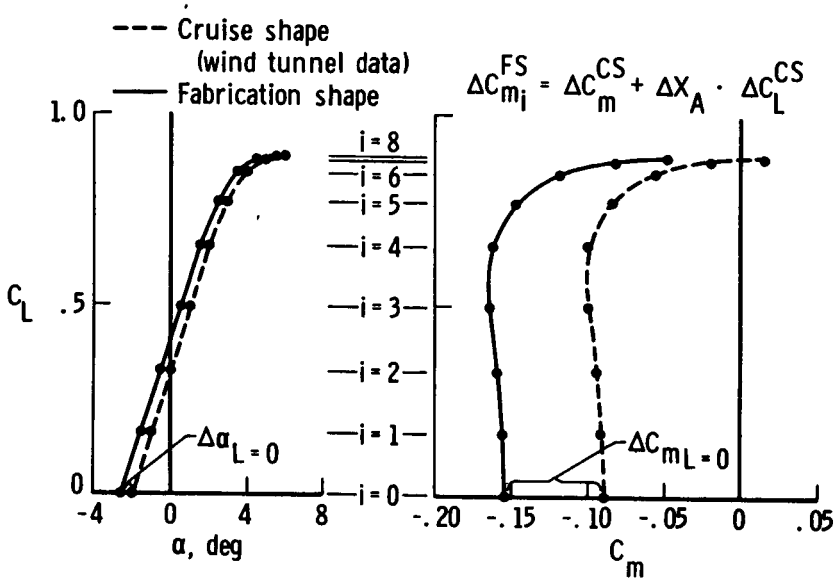

Figure 11.-Procedure for using analysis results to modify wind tunnel data.

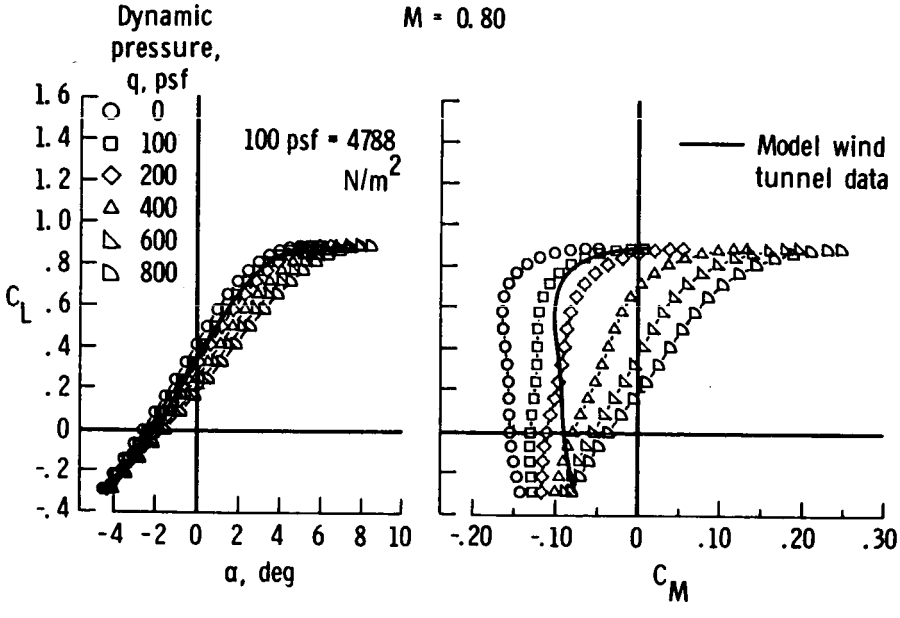

Figure 12.-Analysis results for the flexible airplane - tail off.

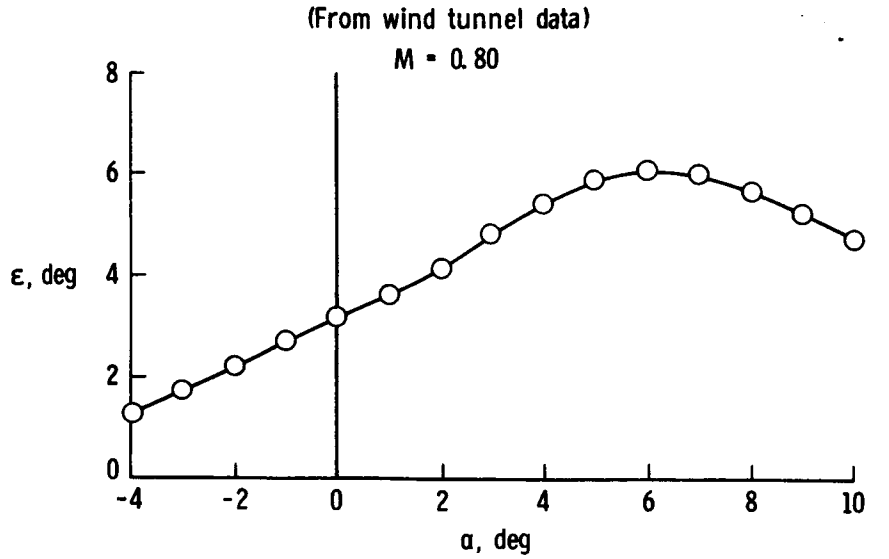

Figure 13.-Downwash at the horizontal tail.

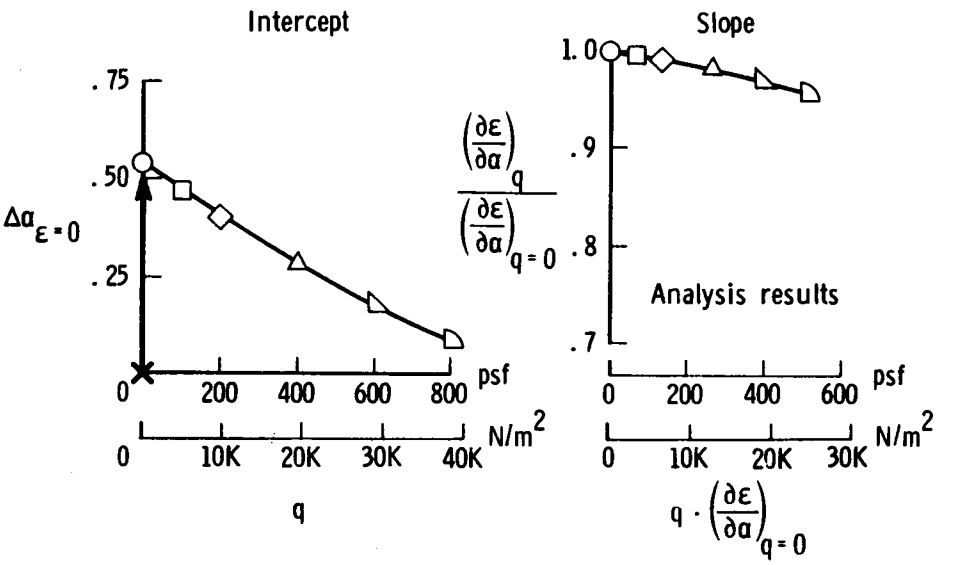

Figure 14.-Changes in downwash at the tail.

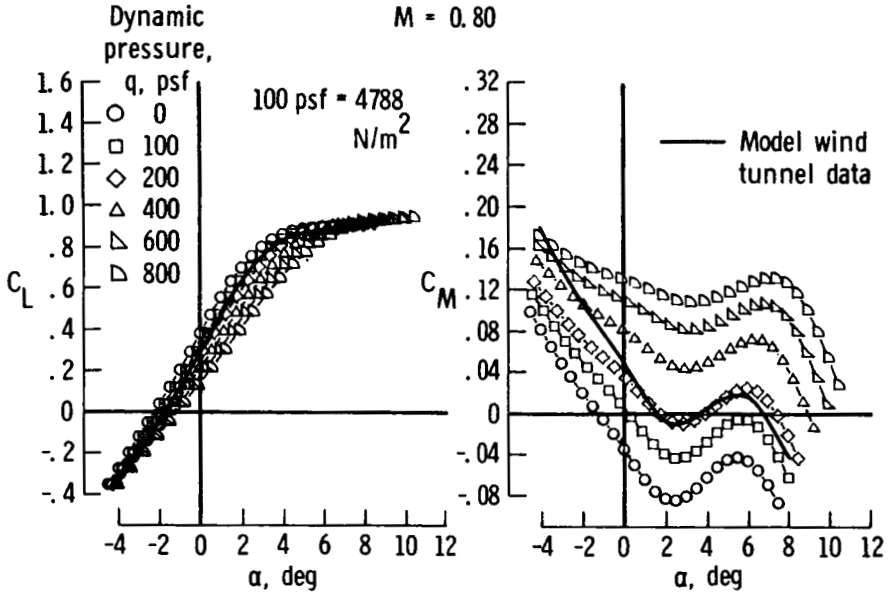

Figure 15.-Flexibility effects for example aircraft.

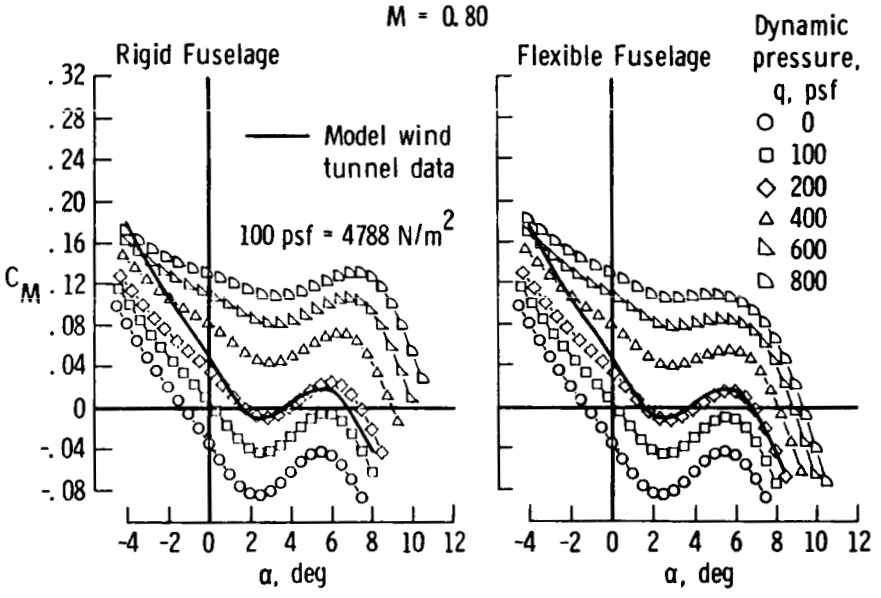

Figure 16.-Effect of fuselage flexibility on pitching moment coefficient.

1. Report No.	2. Government Accession No.	3. Recipient's Catalog No.
NASA TM-89060		

4. Title and Subtitle	5. Report Date
Prediction of Wing Aeroelastic Effects on Aircraft Lift and Pitching Moment Characteristics	October 1986
	6. Performing Organization Code 505-63-21-04
7. Author(s)	8. Performing Organization Report No.
Clinton V. Eckstrom	
9. Performing Organization Name and Address	10. Work Unit No.
NASA Langley Research Center Hampton, VA 23665-5225	11. Contract or Grant No.
12. Sponsoring Agency Name and Address	13. Type of Report and Period Covered
National Aeronautics and Space Administration Washington, DC 20546	Technical Memorandum
	14. Sponsoring Agency Code

15. Supplementary Notes

Presented at AGARD Specialists Meeting on Static Aeroelastic Effects on High Performance Aircraft, Athens, Greece, October 1-2, 1986.

16. Abstract

The distribution of flight loads on an aircraft structure determine the lift and pitching moment characteristics of the aircraft. When the load distribution changes due to the aeroelastic response of the structure, the lift and pitching moment characteristics also change. An estimate of the effect of aeroelasticity on stability and control characteristics is often required for the development of aircraft simulation models for evaluation of flight characteristics. This presentation outlines a procedure for incorporating calculated linear aeroelastic effects into measured nonlinear lift and pitching moment data from wind tunnel tests. Results are presented which were obtained from applying this procedure to data for an aircraft with a very flexible transport type research wing. The procedure described is generally applicable to all types of aircraft.

17. Key Words (Suggested by Author(s))	18. Distribution Statement
Aeroelastic Stability and Control Lift and Pitching Moment	Unclassified - Unlimited Subject Catagory 08

19. Security Classif. (of this report)	20. Security Classif. (of this page)	21. No. of Pages	22. Price
Unclassified	Unclassified	18	A02

N-305

For sale by the National Technical Information Service, Springfield, Virginia 22161